Materials Science and Engineering A 527 (2010) 6235–6238

Contents lists available at ScienceDirect

Materials Science and Engineering A

journal homepage: www.elsevier.com/locate/msea

Effects of local phase conversion on the tensile loading of pulsed Nd:YAG laser processed Nitinol

M.I. Khan*, Y. Zhou[1]

Department of Mechanical Engineering, University of Waterloo, 200 University Avenue West, Waterloo, Ontario N2L-3G1, Canada

ARTICLE INFO

Article history:
Received 23 February 2010
Received in revised form 31 May 2010
Accepted 10 June 2010

Keywords:
Laser processing
Nitinol
Shape memory alloys (SMA)
Tensile properties
Pseudoelasticity

ABSTRACT

The unique material properties of Nitinol, such as its shape memory effect, pseudoelasticity and biocompatiblility, make it ideal for medical device applications. However, reported adverse effects during laser processing of Nitinol have severely impeded its deployment. The current article details some key findings associated with local phase conversion resulting from pulsed Nd:YAG laser processing of Nitinol (Ni-49.2 at.% Ti). Results revealed changes to room temperature phases of the processed metal when compared to the base material, which also affect the tensile properties of Nitinol.

1. Introduction

The excellent biocompatibility coupled with good strength and ductility has made Nitinol an attractive candidate for medical device applications. Laser processing (i.e. surfacing, ablation, welding, etc.) is a key fabrication step in the manufacture of many miniature devices. However, difficulties associated with reduced mechanical performance after laser processing has obstructed its implementation in many vital components. Some of these issues have been detailed in two separate publications, by Falvo et al. and Chau et al., both of which have expressed a need for further research before practical applications of NiTi can commence [1,2]. Hence, research detailing the effects of laser processing on Nitinol is essential to overcome many of these challenges.

Nitinol's functional properties are largely linked to its ability to reversibly transform from low temperature martensite to high temperature austenite. However, existing publications on laser welding have mainly focused on the mechanical performance with results being very preliminary. For example, Schloßmacher et al. showed laser welded Ni-rich Nitinol to have relatively improved tensile strength, with the retention of pseudoelastic properties [3]. Contradictory results were presented by Tuissi et al. in a later study that showed Ni-rich Nitinol to have a decrease in pseudoelastic properties [4]. Detailed analysis of structural and phase changes is still required in order to better understand the influence of laser processing on mechanical performance. In particular, the tensile properties of the low temperature martensite phase are substantially different from the high temperature austenite phase, which typically exhibits reversible stress-induced transformation (pseudoelasticity). However, publications have thus far shown minimal effect of laser processing on these discrete transformation temperatures, including studies by Schloßmacher et al. [3], Tuissi et al. [4], and Flavo et al. [1]. These all reported only minor increases in transformation temperature whereas Hsu et al. [5] showed a slight decrease. None of the aforementioned changes to transformation temperature were stated to be severe enough to alter the weld mechanical performance.

The aim of the current study is to illustrate and detail the effects of laser processing of Nitinol on the stable room temperature phase. The effects of phase changes on tensile properties have also been examined. Analysis of the effects of process parameters on the mechanical performance has been presented in a separate publication [6].

2. Experimental methods

2.1. Material

Commercially available SE508 Nitinol strip 0.37 mm thick was used in this study. The chemistry for this particular alloy was 55.8 wt.% Ni and 44.2 wt.% Ti with maximum oxygen and carbon contents of 0.05 wt.% and 0.02 wt.%, respectively. The as-received

* Corresponding author. Tel.: +1 416 300 6616; fax: +1 519 888 6197.
E-mail addresses: ibraheem@rogers.com (M.I. Khan), nzhou@uwaterloo.ca (Y. Zhou).
[1] Tel.: +1 519 888 4567x36095; fax: +1 519 888 6197.

0921-5093/$ – see front matter © 2010 Elsevier B.V. All rights reserved.
doi:10.1016/j.msea.2010.06.025

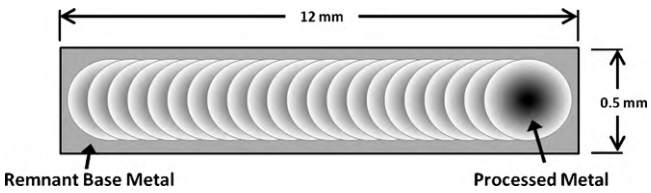

Fig. 1. Schematic of DSC sample.

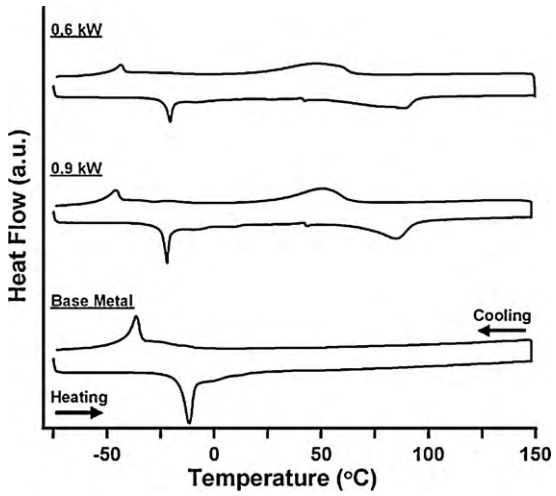

Fig. 2. DSC scans for base and processed metal.

cold-rolled material was heat treated for 1 h at 800 °C to attain transformation and pseudoelastic properties. A dilute solution of hydrofluoric and nitric acid was used to remove the black oxide before laser processing commenced.

DSC analysis was conducted using a Thermal Analysis Q2000 system equipped with a refrigerated cooling system (RCS). DSC curves were recorded in a temperature range from −75 °C to 150 °C using a controlled heating and cooling rate of 5 °C/min. Peak onsets were measured using TA Universal Analysis software (version 4.5). Fig. 1 shows a schematic of the test specimens used for DSC measurements, which were carefully extracted using an Acutome 50 precision saw with a ± 0.01 mm tolerance. The sample size was approximately 0.5 mm × 12 mm and subsequently cut into smaller strips in order to fit into the DSC pans. However, due to the small specimen dimensions, samples contained remnant un-melted material including any heat affected region and base metal.

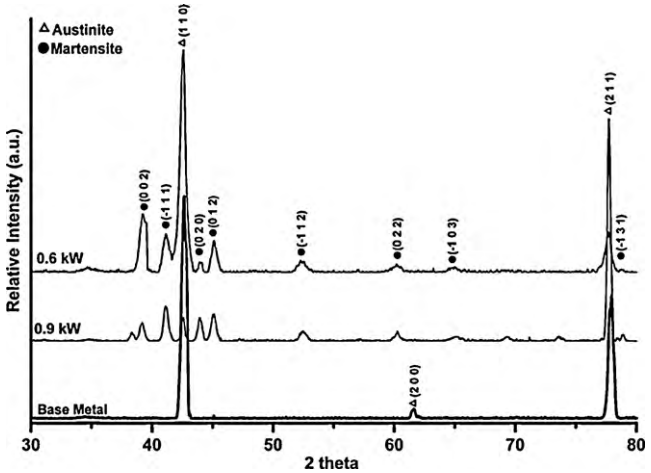

Fig. 3. Room temperature XRD data for processed and base metal.

2.2. Equipment and parameters

Samples were produced using a Myachi Unitek pulsed Nd:YAG laser system (Model LW50 A) which produces a beam with a 1.06 μm wavelength. This particular system is equipped with a power monitor allowing for accurate in-situ assessment of incident power output. Processing was conducted on monolithic sheets. Top and bottom shielding of argon was implemented to avoid oxidation; a flow rate of 30 CFH was selected, as per a previous study on titanium alloys [7]. Minimum peak power criteria included full penetration and 80% pulse spot overlap. Samples were produced using a 400 μm spot diameter with a 3 ms pulse time at 0.6 KW peak beam power and a frequency of 10 pulses per second.

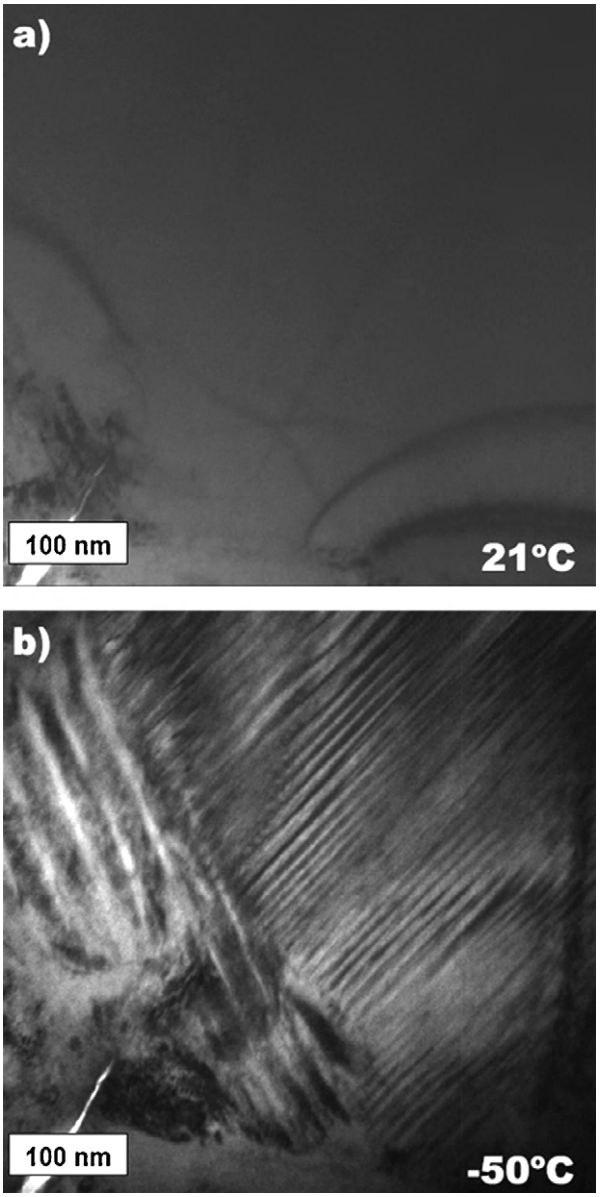

Fig. 4. Base metal TEM microstructure.

2.3. Phase analysis

XRD analysis was carried out using a Rigaku MSC micro-XRD. This particular XRD used a Cu k-alpha x-ray source providing a 1.54 Å wavelength. The selected collimator spot size (0.5 mm) mainly encompassed the processed (re-melted) region with some remnant base metal also being tested. Data conditioning was performed using the JADE software which accompanied the XRD equipment.

Transmission electron microscopy (TEM) was carried out with a Philips CM12 microscope at 120 KeV accelerating voltage. Hot and cold stages were implemented to permit control of phase transformation. TEM sample preparation was conducting using a Fischione ion milling system at −90 °C to minimize heat-induced artefacts.

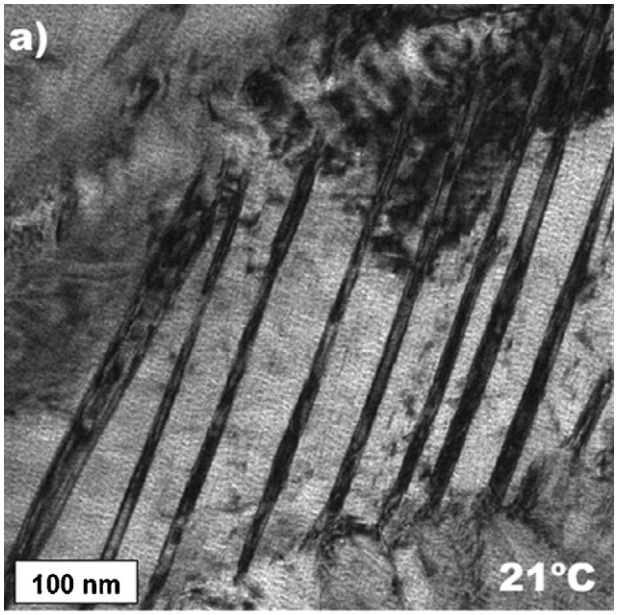

Fig. 5. 0.6 kW processed metal TEM microstructure.

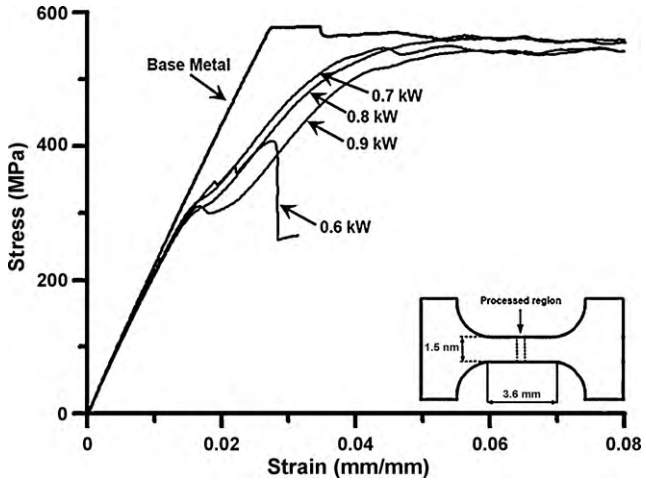

Fig. 6. Stress–strain curve for pseudoelastic region.

Table 1
Peak onset for DSC scans.

	Low temp. transformation				High temp. transformation			
	A_s	A_f	M_s	M_f	A_s	A_f	M_s	M_f
0.6 kW	−21.3	−16.5	−39.6	−47.3	72.9	96.4	66.2	22.0
0.9 kW	−20.1	−14.7	−37.7	−48.8	70.9	89.3	62.6	22.0
BM	−16.1	−8.6	−33.2	−44.2	Not present			

3. Results and discussion

Differential scanning calorimetry curves for the processed and base material are shown in Fig. 2, with quantified peak onsets provided in Table 1. Base metal results indicated room temperature phases to consist of predominately austenite. In comparison, the processed samples exhibited multiple transformation peaks, including a pair of high temperature and low temperature peaks. Residual un-melted material on these samples after cutting could account for the low temperature peaks, which also have transformation temperatures similar to the base metal. However distinct high temperature peaks were also present, suggesting the occurrence of a separate transformation.

Additional DSC peaks are typically observed in cold worked or aged Nitinol during R-phase transformation. However during the presence of R-phase, an intermediate transformation would produce a peak between austenite and martensite during cooling [8]. The present data shows two distinct transformation peaks outside of that range. In addition, the fully annealed base material did not show any presence of R-phase transformation, due to preservation of the solid solution by quenching to room temperature. These additional peaks suggest the presence of multiple phase transformations, including a low temperature (< room temperature) and high temperature (> room temperature) transformation.

Grain coarsening has been shown to slightly lower transformation temperatures of Nitinol alloys [9]. Materials that have undergone laser processing often contain a heat affected zone (HAZ) where grain coarsening is commonly experienced. This is more prominent in materials originally having a small grain structure induced by thermo-mechanical processing during the manufacturing stages. This was observed by Ogata et al. who showed increased grain size in the HAZ region after laser processing of heavily cold worked NiTi alloys [10]. However, in the present study the annealing procedures carried out prior to laser processing retained a relatively large base metal grain structure; such that, HAZ coarsening was not detectable in the microstructure. Influences of HAZ coarsening on transformation temperatures were expected to

be removed due to the annealing procedures. Furthermore, transformation temperatures showed a distinct increase in temperature, which is contrary to the effects observed in coarsening.

Room temperature (21 °C) XRD data showing indexed peaks for the base and processed material are shown in Fig. 3. As expected from the DSC results, base metal peaks identified the sole presence of the cubic austenite phase. Conversely, both austenite and martensite phases were detected in the laser processed samples. This result corroborated well the DSC data, which showed complete transformation to austenite for the processed metal peaks to finish at 89.3 °C, well above room temperature (Table 1). It should be mentioned that the additional unlabeled faint peaks in Fig. 3 (i.e. near 35°, 57°, 69°, and 74°) within the processed metal also corresponded to martensite, as determined by the referenced work [11].

Detailed phase characterization facilitated by TEM analysis further confirmed the local phase alteration due to laser processing. First, base metal TEM microstructure was observed at 21 °C and −50 °C at the same site, shown in Fig. 4a and b, respectively. Decreasing sample temperature demonstrated the transformation from simple cubic austenite to twinned martensite. Room temperature TEM observation of the representative 0.6 kW processed metal, shown in Fig. 5a, confirmed the presence of twinned martensite. Fig. 5b shows the effect of subsequent heating of the sample to 100 °C that induced the solid state transformation into simple cubic austenite. Hence, observations show laser processed material exhibiting higher transformation temperature when compared to the original base metal.

A previous study detailing the tensile properties of laser processed Nitinol revealed an 'initial plateau' during the elastic loading of the bulk austenite in the gauge length [6]. This effect, shown in Fig. 6, became more prominent as peak power increased, which resulted in an increased width of the processed region within the gauge length. However during cyclic loading the 'initial plateau' was not present after the first loading cycle and resulted in a larger permanent residual strain [6]; hence, plastic deformation of the local material was suspected. Current results confirmed this by showing a local phase conversion from austenite to martensite induced by laser processing. Consequently the tested tensile gauge length (shown in Fig. 6) contains local martensite, where processing was conducted, and austenite from the unprocessed base material. It is believed that subsequent tensile loading would first induce detwinning of the local twinned martensite; followed by stress-induced martensite transformation (pseudoelastic) of the remaining gauge length. Hence, the previously observed yielding and larger permanent residual strain during cyclic loading can be attributed largely due to detwinning of the local martensitic region.

Compared to published research, current results reveal substantial changes to local transformation temperatures induced by pulsed Nd:YAG laser processing. In particular the stable room temperature phase was converted from austenite to martensite. Thus, these results are contradictory to those observed by Hsu et al. who reported a slight decrease in transformation temperature after CO_2 laser welding of Nitinol [5]. A detailed understanding of microstructural and phase changes induced by welding is critical to the design and fabrication of medical devices; particularly when shape memory or good mechanical performance is required. Transformation temperatures are known to be largely affected by thermo-mechanical processing and Ti/Ni ratio [8] both of which can be experienced during laser welding due to the experienced thermal cycles and local vaporization, respectively. However the specific mechanisms responsible for the changes detailed in the current study are not fully understood. Therefore, further detailed investigation on the mechanism responsible for phase alteration and methods to either minimize or control these effects is still required.

4. Summary

The current study analyzed the effects of laser processing on the transformation temperature of Nitinol. DSC results revealed additional high temperature transformation peaks that can be attributed to the local phase conversion induced by laser processing. These results were further corroborated with room temperature XRD analysis, showing only austenite in the base metal and added martensite peaks in the melted metal. TEM observations confirmed the presence of room temperature martensite within the processed/melted zone. Finally, these local modifications need to be considered in the design and fabrication of devices implementing laser processed Nitinol.

Acknowledgement

The authors would like to acknowledge the support of NSERC. The authors are also grateful to Andreas Wick of the Nitinol Devices and Components (NDC) for providing the material examined in this study.

References

[1] A. Falvo, F.M. Furgiuele, C. Maletta, Mater. Sci. Eng. A 412 (1–2 (5 December)) (2005) 235–240.
[2] E.T.F. Chau, C.M. Friend, D.M. Allen, J. Hora, J.R. Webster, Mater. Sci. Eng. A 438-440 (2006) 589–592.
[3] P. Schloßmacher, T. Haas, A. Schüßler, Laser welding of Ni-rich TiNi shape memory alloy: Pseudoelastic properties, in: A.R. Pelton, D. Hodgson, S. Russell, T.W. Duerig (Eds.), SMST-97, Proc. 2nd Intl. Conf. on Shape Memory and Superelastic Technologies, MIAS, Monterey, CA, 1997, pp. 137–142.
[4] A. Tuissi, S. Besseghini, T. Ranucci, F. Squatrito, M. Pozzi, Mater. Sci. Eng. A A273–275 (15 December) (1999) 813–817.
[5] Y.T. Hsu, Y.R. Wang, S.K. Wu, C. Chen, Metall. Mater. Trans. A 32A (3 (March)) (2001) 569–576.
[6] M.I. Khan, S.K. Panda, Y. Zhou, Mater. Trans. 49 (11) 2702–2708.
[7] X. Li, J. Xie, Y. Zhou, J. Mater. Sci. 40 (13) 3437–3443.
[8] K. Otsuka, C.M. Wayman, Shape Memory Materials, Cambridge University Press, Cambridge, UK, 1999, pp. 53–58.
[9] F.J. Gil, J.M. Manero, J.A. Planell, J. Mater. Sci. 30 (10) 2526–2530.
[10] Y. Ogata, M. Takatugu, T. Kunimasa, K. Uenishi, K.F. Kobayashi, Mater. Trans. 45 (4 (April)) (2004) 1070–1076.
[11] Y. Kudoh, M. Tokonami, S. Miyazaki, K. Otsuka, Acta Metall. 33 (11) 2049–2056.